

The Cosmic Web Imager : An integral field spectrograph for the Hale Telescope at Palomar Observatory. Instrument design and first results.

Mateusz Matuszewski^a, Daphne Chang^a, Robert M. Crabill^a, D. Christopher Martin^a, Anna M. Moore^b, Patrick Morrissey^a and Shahinur Rahman^a

^aSpace Astrophysics Laboratory, Caltech MC 208-17, Pasadena, CA 91125

^bCaltech Optical Observatories, Caltech MC 11-17, Pasadena, CA 91125

ABSTRACT

We describe the Cosmic Web Imager (CWI), a UV-VIS integral field spectrograph designed for the Hale 200" telescope at the Palomar Observatory. CWI has been built specifically for the observation of diffuse radiation. The instrument field of view is 60"×40" with spectral resolving power of $R \sim 5000$ and seeing limited spatial resolution. It utilizes volume phase holographic gratings and is intended to cover the spectral range 3800Å to 9500Å with an instantaneous bandwidth of ~ 450 Å. CWI saw first light in July 2009, and conducted its first successful scientific observations in May 2010.

Keywords: Cosmology, Integral Field Spectroscopy, VPH Gratings, Cosmic Web Imager

1. THE COSMIC WEB IMAGER INSTRUMENT

1.1. CWI Mission

The Cosmic Web Imager's primary objective is to use line emission from hydrogen ($\text{Ly}\alpha$ 1216Å), carbon (CIV 1550Å), and oxygen (OVI 1036Å) to detect and map diffuse gas around and between galaxies and quasars at redshifts $2 < z < 6$. Measuring the strength, and mapping the extent, of this emission will give a better understanding of the interactions between forming and evolving galaxies and their surroundings. It will help clarify the origin and nature of the Lyman- α blobs already observed using narrowband imaging¹ and lower resolution spectroscopy.^{2,3} This mapping can also reveal the dim filamentary and sheet structure permeating the universe, the so-called cosmic web, which has not yet been directly observed.^{4,5} The CWI combination of ample field of view, moderate resolution, coupled with a relatively high throughput and good noise and background subtraction characteristics, also make the instrument very suitable for studying other diffuse objects, such as light echoes from supernovae, star-forming regions in low surface brightness galaxies, post-merger tidal tails, or superwinds in nearby galaxies, just to name a few.

1.2. CWI Characteristics

The Cosmic Web Imager is a UV-VIS integral field spectrograph mounted at the Cassegrain focus of the Hale 200" telescope at the Palomar Observatory. The field of view is 60"×40"; this is well suited to volumes around galaxies and is commensurate with what the characteristic sizes of the $\text{Ly}\alpha$ blobs. The instrument spatial resolution is seeing limited ($\sim 1''$) in the short direction (along the slices), and slit limited ($\sim 2.5''$) in the long direction (across the slices). As the field of view can be rotated on the sky, it is possible to construct a seeing-limited image using multiple exposures covering the same objects at different instrument orientations. CWI has an anticipated wavelength coverage from 3800Å to 9500Å with resolving power $R = \lambda/\Delta\lambda \geq 5000$ ($\Delta v \leq 60\text{km/s}$). At the time

Further author information: (Send correspondence to M.M.)

M.M.: matmat@caltech.edu, Tel.: (626) 395 1879

D.C.M.: cmartin@srl.caltech.edu

P.M.: patrick@srl.caltech.edu

A.M.M.: amoore@astro.caltech.edu

S.R.: shanin@caltech.edu

Ground-based and Airborne Instrumentation for Astronomy III, edited by Ian S. McLean,
Suzanne K. Ramsay, Hideki Takami, Proc. of SPIE Vol. 7735, 77350P · © 2010
SPIE · CCC code: 0277-786X/10/\$18 · doi: 10.1117/12.856644

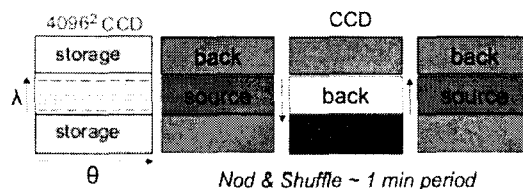


Figure 1.1. In the nod-and-shuffle mode, the top and bottom thirds of the detector are masked off. Only the central region is used for observation. The instrument is pointed at a source field, and after a short period, on the order of a few minutes, the charge is shuffled on the CCD to one of the storage areas and the telescope is noddied toward a nearby background field. This process is repeated several times until the detector is read out. Switching between source and background more frequently than in the full-detector mode improves the level of sky subtraction, critical to observing emission from diffuse sources.

Parameter	Value
Field of view	60" \times 40"
Spatial resolution	Slit ($\sim 2.5''$) \times Seeing ($\sim 1''$) Limited
Wavelength coverage	λ : 3800Å to 9500Å
Instantaneous bandpass	$\Delta\lambda$: 450Å(150Å)
Spectral resolution	$R \geq 5000$
Instrument efficiency	Peak $\sim 27\%$
Detector read noise	$\sim 2e$
Limiting sensitivity*	10^{-18} erg cm $^{-2}$ s $^{-1}$ arcsec $^{-2}$

Table 1.1. A highlight of the main CWI parameters. The limiting sensitivity was calculated for a line-emission signal extended over 600 arcsec 2 on the sky (quarter of the CWI field of view), for a 16h integration; half the time is spent on the science target, other half on a background field. This value assumes sky background subtraction residuals at the 1% level. Improving on this subtraction by a factor of 10 to 100, which the nod-and-shuffle technique and instrument flexure compensation can help do, improves the sensitivity by over an order of magnitude. As a reference, the two brightest Ly α blobs observed by Steidel¹ in the SSA22a field have surface brightness $\sim 5 \times 10^{18}$ erg cm $^{-2}$ s $^{-1}$ arcsec $^{-2}$. See Section 1.2 for discussion of the instrument parameters.

of writing only one of the suite of five gratings is available, limiting the wavelength coverage to $4400\text{\AA} < \lambda < 5600\text{\AA}$. 450Å of this range can be seen at once when the full detector is used for an observation, but only 150Å is available when the instrument is in the nod-and-shuffle configuration (see Figure 1.1). Thanks to the low ($2e^-$) read noise of the detector, CWI becomes sky-background limited (rather than detector-background limited) for integrations longer than ~ 300 s.

2. CWI DESIGN

2.1. Instrument Layout

The optical and mechanical layouts of the Cosmic Web Imager are shown in Figures 2.2 and 2.3. The F/16 telescope beam is intercepted by a flat pick-off mirror (FM1) that redirects it through an astronomical filter toward the image slicer at the focal plane of the telescope. A rectangular 24mm \times 16mm (60" \times 40") image is reformatted into a staggered long slit by an array of pupil mirrors. The light is reflected off a second folding flat (FM2) onto a mirror with a radius of curvature of 4800mm that collimates the beams to 150mm diameter. FM2 has a range of motion of $\pm 2''$ along the direction of the beam and is the primary focusing mechanism internal to the instrument. The now-collimated beams are directed toward a third folding flat (FM3) that reflects them through an opening onto the underside of the bench. The light reflects off a fourth folding flat (FM4) that sends it parallel to the bottom bench surface, forming a pupil near the transmissive diffraction grating. The periscope-like arrangement of FM3 and FM4 has the effect of orienting the long-slit perpendicular to the bench and the

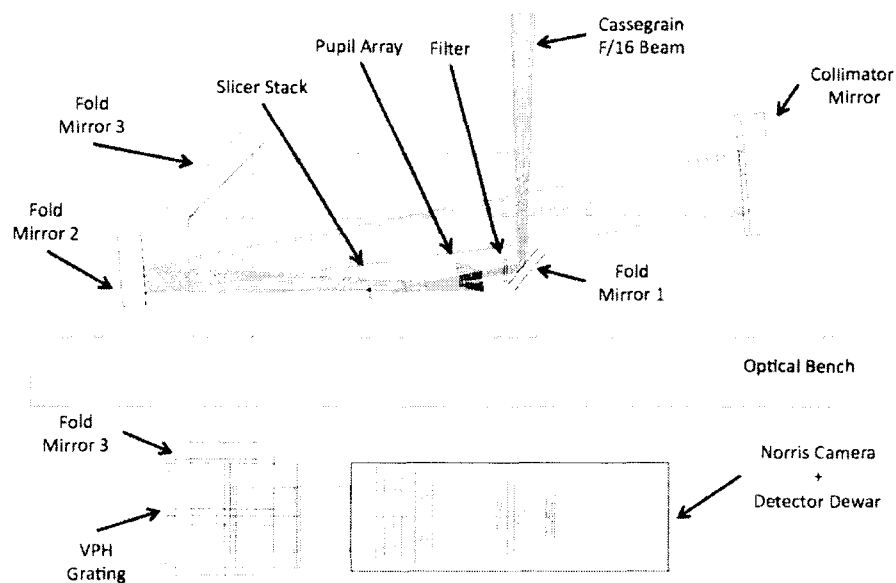


Figure 2.2. A schematic view of the CWI optical path. See Section 2.1 for more details.

dispersion direction parallel to it. An actuated tilt mechanism in FM3 and FM4 can be used to counteract the effects of flexure within the instrument. The VPH grating, operating near the Bragg condition disperses the beams toward the legacy Norris lens. The high performance optic focuses the spectra onto a low noise E2V 231-84 CCD. The grating and camera-dewar assembly are mounted so as to be able to rotate about a common pivot point at the center of the grating, allowing for the selection of the wavelength range to be observed. FM1 can be moved out of the way to let a beam from a telescope simulating calibration unit to enter the spectrograph. Additionally, a pair of pick-off flats offset from the main telescope axis sends a (roughly) $3' \times 3'$ portion of the focal plane of the telescope to a guider camera.

2.2. Integral Field Unit

The CWI Integral Field Unit consists of an image slicer, made of 24 1mm thick, 16mm wide individually manufactured aluminum blocks and an array of 24 pupil mirrors (12 each of $21 \times 32 \text{ mm}^2$ and $23 \times 36 \text{ mm}^2$). The slicers were designed at Caltech, manufactured and assembled by the Kugler Corporation. The front surface of each element is flat and has been machined to a specific tip-tilt compound angle, to an 0.1° tolerance. The optical surfaces were diamond-turned to a surface roughness of under 7nm rms and given an enhanced aluminum reflection coating. The telescope beam comes to a focus at the slicer and the $60'' \times 40''$ field of view is redirected onto the brickwall configuration array of pupil mirrors. These elements reimagine the rectangular field of view into a 465mm long staggered virtual slit that has a slight upward curvature (see Figure 2.4). Each pupil mirror is attached to a solid aluminum backplate via a specially designed flexure mount. The entire IFU is tilted at 10° with respect to the bench to reduce vignetting and allow for improved baffling. The IFU was aligned relying on mechanical tolerances and using the tip-tilt pupil mounts to correct the locations of the slices on the detector, removing any overlaps.

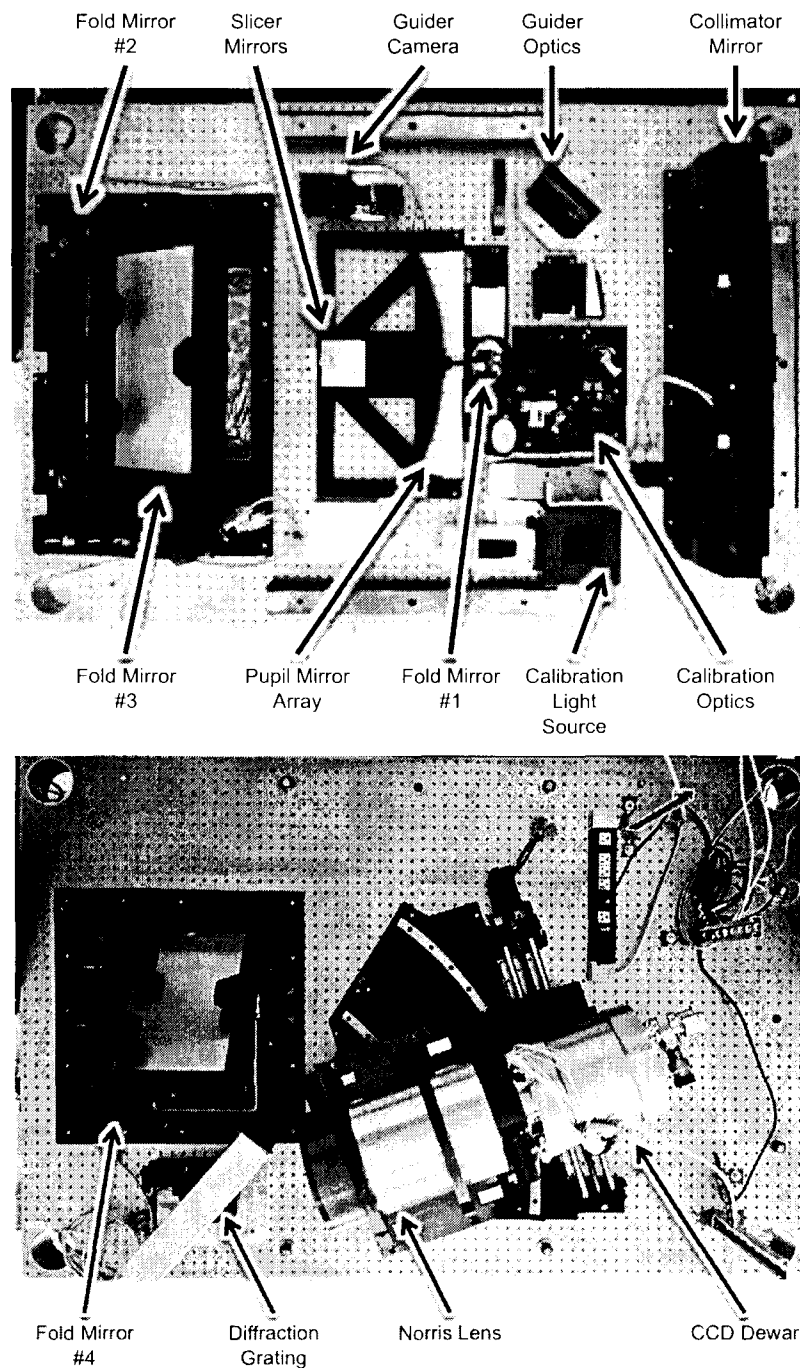


Figure 2.3. Photographs of the two sides of the 6' x 4' CWI bench. The top picture was taken from roughly the same angle as the Palomar beam enters the instrument, and thus reflection of the slicer is visible in Fold Mirror #1. The guider camera and guider optics (two folding flats and a 6" field lens) are visible toward the top of the image. The calibration unit occupies the space in the bottom right of the photo and is further explained in Section 2.6. The bottom side of the bench, in addition to the objects shown, also houses shutter and motor controllers as well as some of the camera readout electronics.

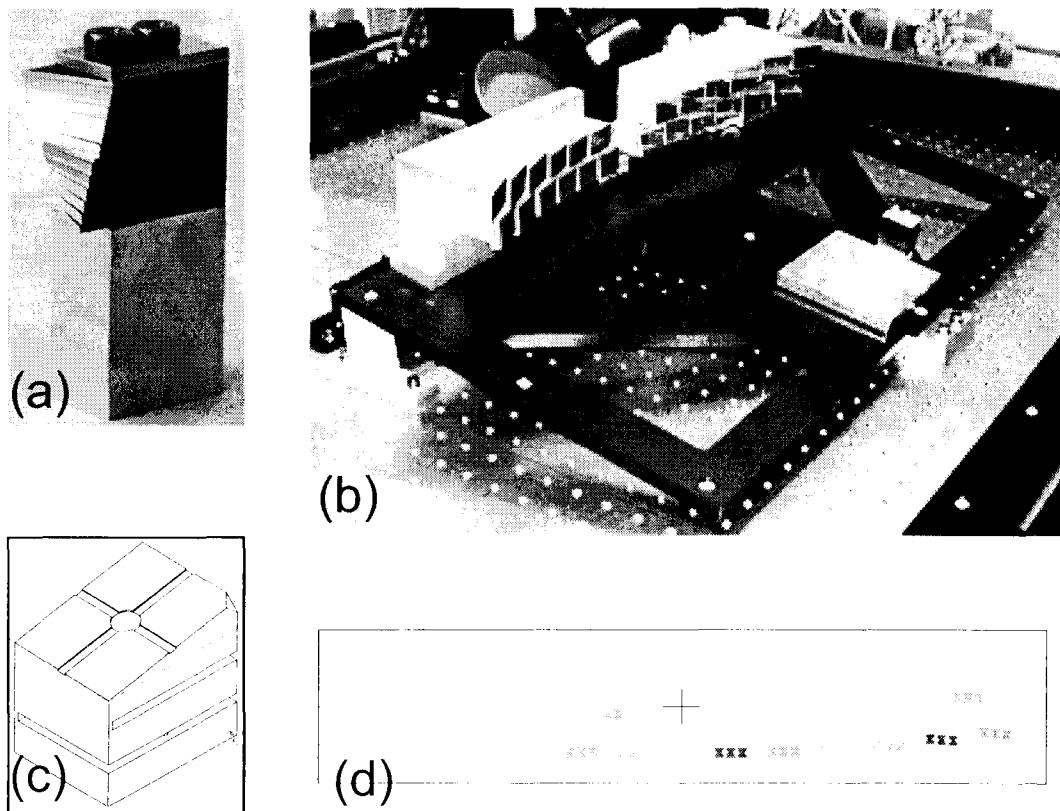


Figure 2.4. The CWI IFU. The slicer stack assembly is shown in figure (a). The slicer mirrors reflect parts of the telescope focal plane toward the pupil mirror array, shown in (b). The pupil mirror centers lie on a hyperboloid surface and are angled so that the images of the slicer mirrors form a virtual slit at the focus of the collimator mirror. The brickwall configuration of the pupil mirrors permits an efficient packing of the spectra on the CCD. There is a slight upward curvature to the pupil mirror arrangement, when it is looked at face-on. This counteracts the conic diffraction that occurs at the grating, thus increasing the total simultaneous wavelength covered by the slices. The resultant 465mm virtual entrance slit to the spectrograph is shown in (c). Figure (d) is a schematic of a flexure mount used to install the pupil mirrors. The glass was bonded to these aluminum blocks using 3M Scotch-Weld 2216 Epoxy; the grooves visible at the top served to channel away the excess bonding agent. The tip-tilt is controlled by two 2-80 fine-threaded screws that set the angle of the flexures. This design gives an angular range of 1.5° in both axes with a resolution better than 0.05° .

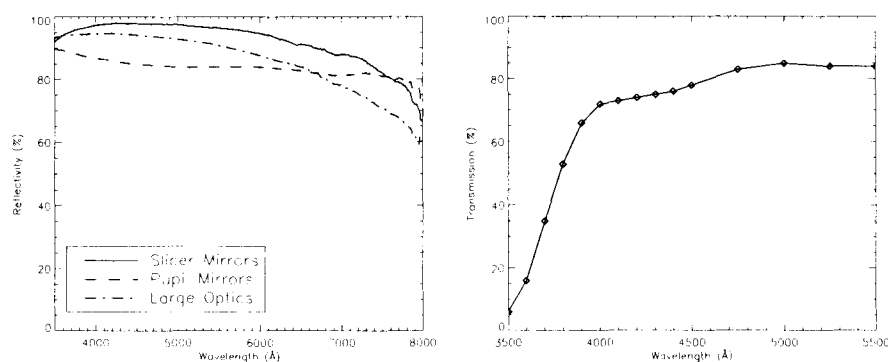


Figure 2.5. Sample measured reflectance curves of the CWI mirrors and the Norris Lens throughput, as measured at Caltech. Replacing the mirror coatings with robust multi-layer silver coatings⁶ is one of the anticipated future improvements to the instrument that could increase the throughput by as much as a factor of 1.5.

2.3. Mirrors and Coatings

The instrument has seven reflective elements, in addition to the two telescope optics. All reflective coatings are protected aluminum optimized to the 4000Å-5000Å range, but, due to differences in materials and vendors, the resultant coatings differ slightly. Figure 2.5 shows several measured reflectivity curves for the CWI optics. The large optics, namely FM1, FM2, FM3, FM4, and the Collimator, were manufactured by Optical Mechanics Inc. The all-metal aluminum slicer mirrors were coated by the assembly vendor, and the BK7 pupil mirrors were given a protected aluminum coating by Custom Scientific, Inc.

With the exception of FM1, which is a 4" diameter round mirror, the remaining large optics are rectangular, FM2 and the Collimator having significantly high aspect ratios. The mounts for these optics were designed at Caltech in collaboration with Newmark Systems and manufactured by the latter. The mirrors are held semi-kinematically in cells via a system of 6 pivoting rubber pads, each opposite a pivoting hard-stop. Three of these are on the front surface, two along the long edge of the mirror and one on the short side. The hard pads that rest on the optical surfaces of the mirrors are flat, with the exception of the collimator pads that were molded to match its radius of curvature. The nitrile rubber pads are compressed to provide a total restoring force of 2.5g along each axis. This value was chosen as a compromise between the force necessary to keep the mirrors fixed in the cells and protect them from damage during transport to and mounting at the telescope, while keeping the stress on the glass low.

2.4. Gratings

CWI is built to employ VPH gratings, although it can accommodate other transmissive or reflective gratings or even a mirror, which would result in an imaging mode. The instrument uses the gratings in the classical Bragg condition configuration, as described in literature.⁷⁻⁹ This arrangement permits tuning the instantaneous bandpass to any 450Å of the wavelengths accessible to a given grating (if the full detector is used; 150Å in the nod-and-shuffle configuration). At the time of writing, CWI is equipped with a single grating manufactured by Wasatch Photonics covering the wavelength range from 4400Å to 5600Å and designed to have its absolute diffraction efficiency maximum at 4900Å. The 3050 lines/mm transmission grating, in conjunction with the 150mm beam size, 1mm slit-width and angles of incidence and diffraction both greater than 45°, yield a spectral resolution of $R \geq \lambda/\Delta\lambda \geq 5000$ for the entire range of the grating, with linear dispersion $\sim 7.5\text{Å/mm}$. As the spectrograph operates near Bragg, there is only minimal anamorphic magnification. Conical diffraction effects are partially taken out with the design of the integral field unit. We measured the grating throughput in lab at the 532nm green laser line and found it to peak at about 70%. Our measurements of the full system throughput both in lab and on sky are consistent with this value.

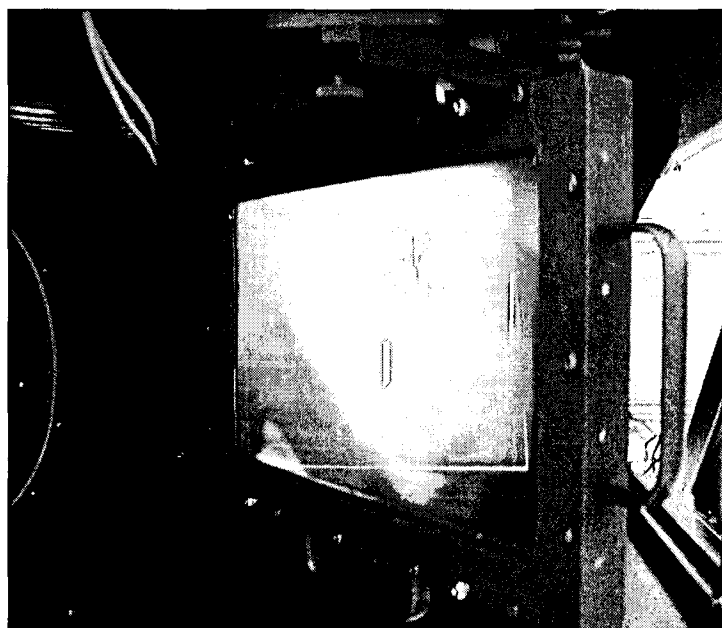


Figure 2.6. CWI green (4400Å-5600Å) grating mounted on a rotating stage via an interface plate that allows for easy manual exchange.

2.5. Camera and Detector

CWI is reusing the Norris Spectrograph lens.¹¹ This optic has good achromatic performance, with a throughput fall-off toward the blue edge of our wavelength range (see Figure 2.5). Bolted onto the back of the lens barrel is a dewar housing a back-illuminated E2V CCD231-84. The 4096x4096 15 μ m pixel device is driven by an ARC Inc. controller and operated using an ArcView and LabView based software suite. The detector runs at T \sim 90°C and exhibits exceptionally low read noise at \sim 2e $^-$ for all four device read-out channels. The CCD has an anti-reflection coating that peaks at \sim 80% between 4000Å and 5000Å. A mask assembly can be attached to the CCD package to block off 2/3 of the device as storage areas for the nod-and-shuffle mode.

2.6. Calibration Unit

The dedicated calibration unit is built to simulate the Hale telescope beam. The design is illustrated in Figure 2.9. An LED continuum and ThAr arc lamp feed a 6" calibration sphere. At the exit port of the sphere is a linear stage that places one of several calibration objects in front of the 1.5" exit port. These include a flat-field aperture, a regular pinhole grid of 100 μ m pinholes on 1mm pitch, and a single 250 μ m pinhole which can be moved to any location within the port. A 250mm focal length lens reimages the selected calibration object onto the slicer. An aperture stop between the calibration objects and the lens is reimaged to form a virtual pupil at the same distance from the slicer stack as the exit pupil of the telescope. Several folding flats route the beams within a compact area of the CWI optical bench. The calibration beam is injected into the instrument by sliding FM1 and replacing it with a pair of flat mirrors in a periscope configuration.

2.7. Guider Camera

Accurate sky and point source subtraction, as well as the nod-and-shuffle observing mode, require that the instrument pointing be repeatable to under an arc-second. To ensure this CWI is equipped with an optical guider. A pair of flat mirrors redirect a part of the telescope beam offset by 10 arc-minutes from the Hale optical

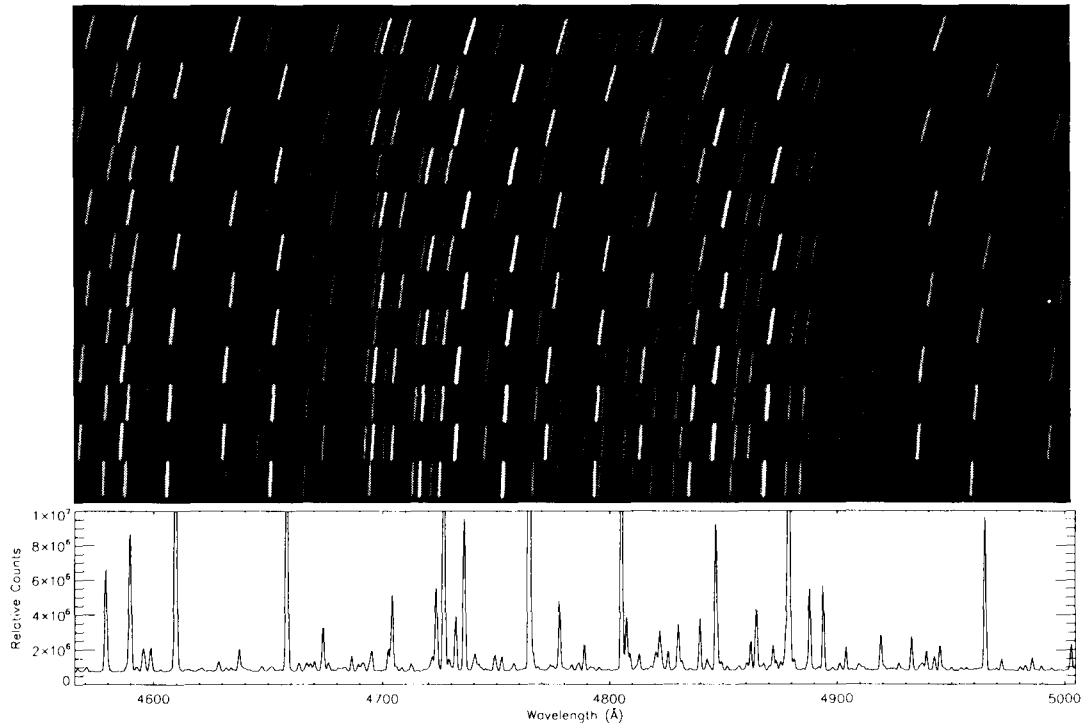


Figure 2.7. One half of the CWI CCD showing 12 of the 24 slices. Notice the $\sim 20\text{\AA}$ offsets between alternating thorium-argon arc-lamp spectra; which is due to the brickwall pattern of the pupil mirrors and corresponding angle variations in the slicer mirrors - this allows for the spectra to be closely packed on the detector. The plot shows the extracted spectrum for the lowest slice in the image after it has been corrected for spatial and spectral nonlinearities.

axis and bring it to a focus at a large format field lens. The light is then focused by an off-the shelf consumer lens onto the image-intensified detector of the Shepherd Autoguider.¹² (This has been used as the guidance system on several Palomar Observatory instruments). The preoptics yield a field of view of $200'' \times 200''$. This is sufficiently large to contain a few stars down to 20th magnitude in the V band.

2.8. Future Plans

CWI saw first light in mid-2009. Although it has performed to specifications, and in certain aspects exceeded our expectations, there is still room for improvement. We intend to add several more gratings and associated filters to be able to cover regions of the full bandpass from 3800\AA to 9500\AA . An upgrade to the mirror coatings would improve the instrument efficiency by close to a factor of 2 at certain wavelengths. It is possible to add a low-resolution ($R \sim 900$) configuration that can capture roughly half of the full instrument bandwidth. We will continue to improve, upgrade and characterize the instrument.

3. FIRST RESULTS

CWI had its first successful science observations over three nights in May 2010. There were two earlier runs in November 2009 and March 2010, but atmospheric conditions prevented meaningful observations. We observed several objects in May, including a quasar, several regions of M82, the ring nebula and a few calibration stars. Figures 3.10 and 3.11 show some of the results.

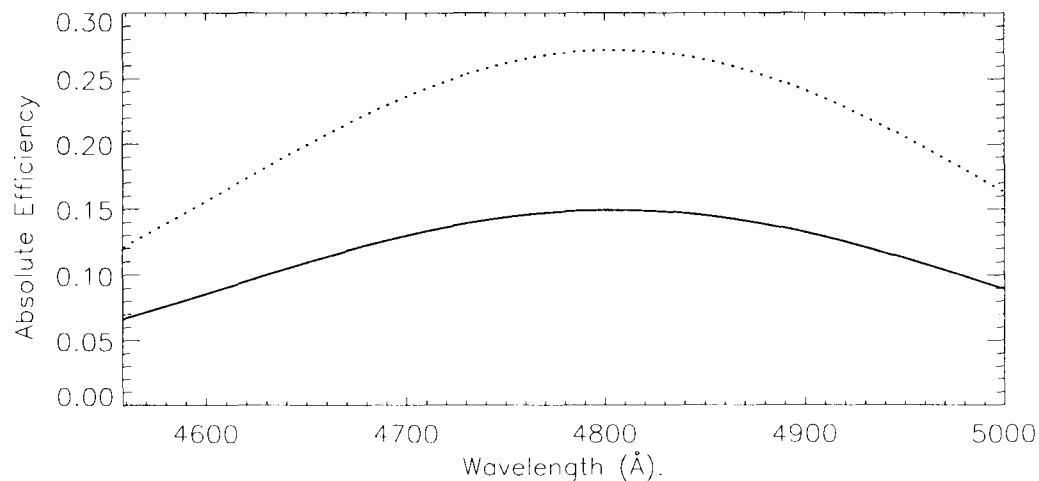


Figure 2.8. Typical CWI instrument throughput for a single slice (solid line), including telescope and atmospheric losses. The curve was obtained from a 30s observation of a calibration standard¹⁰ star BD+28 4211. Taking into account telescope mirror reflectivity of $\sim 85\%$ for the two Hale optics and atmospheric extinction $A(V) \sim 0.3$ gives an estimate for the instrument throughput (dotted line).

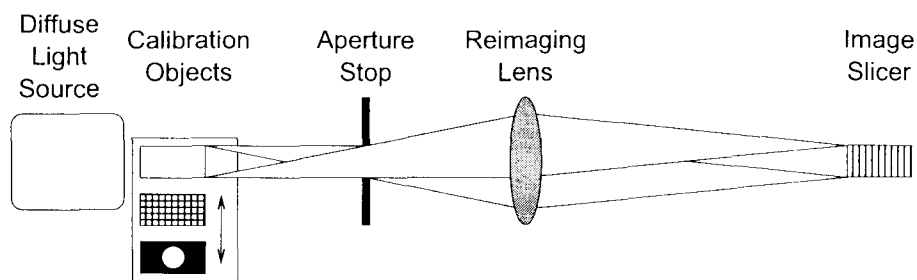


Figure 2.9. CWI Calibration Unit Schematic. An LED continuum source and ThAr line source feed a 6" integrating sphere. Different calibration objects can be placed at the exit port of the sphere. These are then reimaged through an aperture stop and a 250mm focal length lens onto the image slicer.

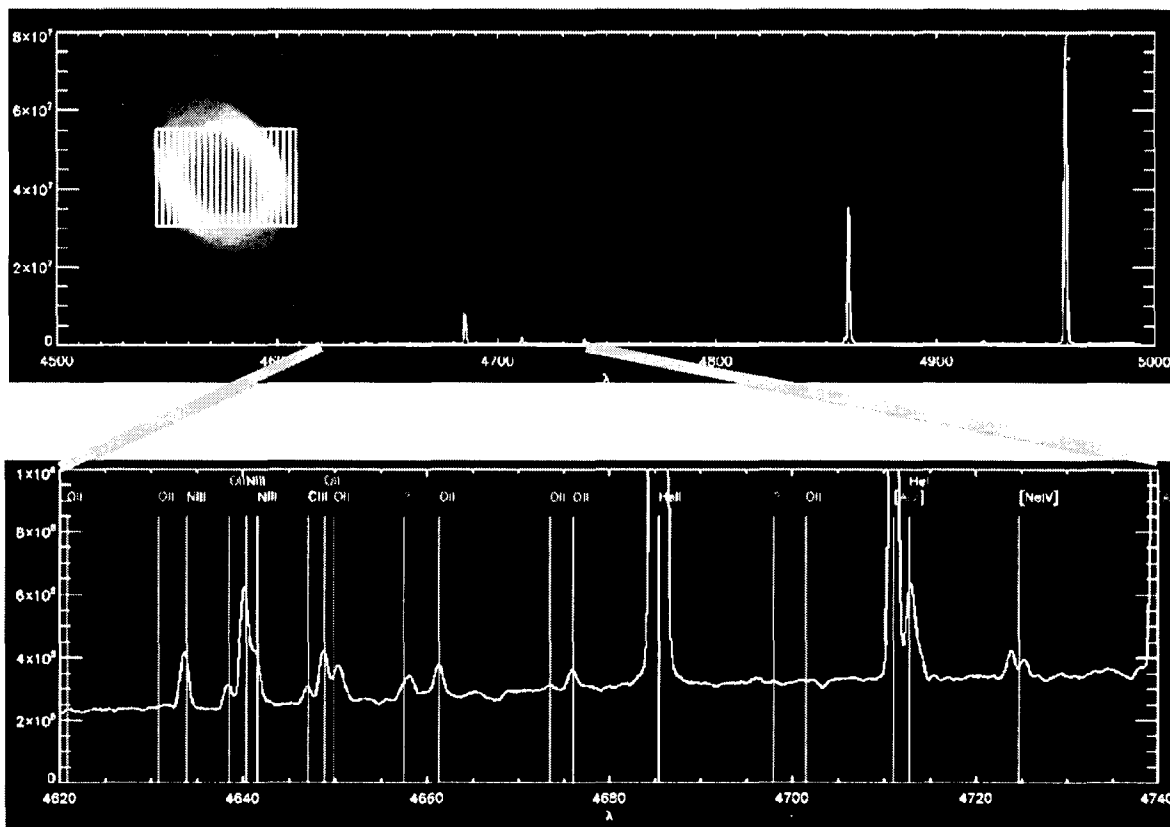


Figure 3.10. CWI took a 10 minute exposure of M57 (Ring Nebula). The orientation of the IFU is shown on the inset overlayed over a Hubble image of the object. The spectrum is generated from coadding the data from the full field. Prominent HeII(4685Å), H β (4863Å) and [OIII](4959Å) are visible. A zoomed view of a subregion shows a zoo of emission lines of various elements, including Oxygen, Helium, Carbon, and Neon. Note that CWI is resolving closely spaced lines, verifying $R \sim 5000$.

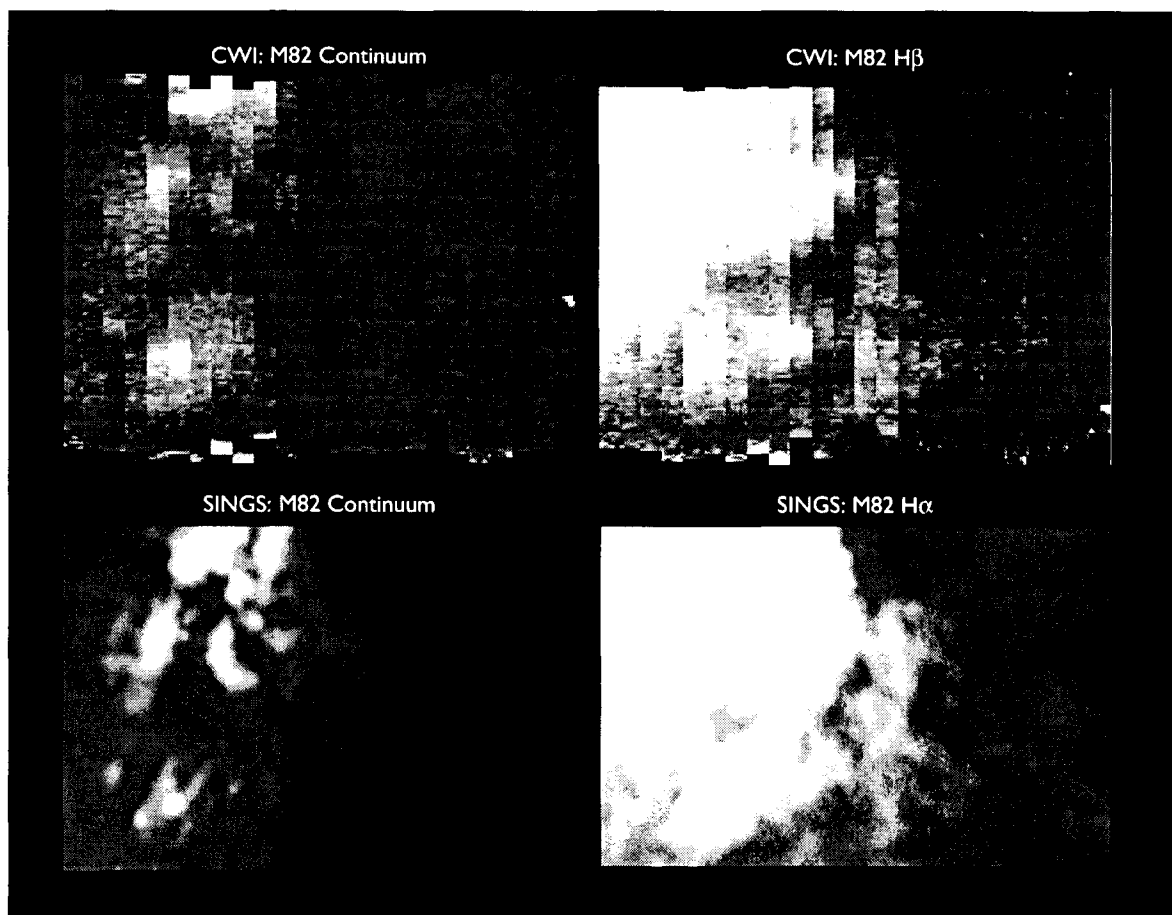


Figure 3.11. A 10 minute exposure of a central region of M82 in both continuum and at $H\beta$ compared with the corresponding continuum and $H\alpha$ images from the SINGS¹³ archive. All images are $60'' \times 40''$. Note the morphological similarities between the two sets of images.

ACKNOWLEDGMENTS

This material is based upon work supported by Caltech and the NSF under Award No. AST-0505381.

We extend special thanks to the wonderful staff at Palomar Observatory and the talented and caring people at Caltech Optical Observatories.

REFERENCES

1. C. C. Steidel, K. L. Adelberger, A. E. Shapley, M. Pettini, M. Dickinson, and M. Giavalisco, "Ly α Imaging of a Proto-Cluster Region at $\langle z \rangle = 3.09$," *Astrophysical Journal* **532**, pp. 170–182, Mar. 2000.
2. R. J. Wilman, J. Geressen, R. G. Bower, S. L. Morris, R. Bacon, P. T. de Zeeuw, and R. L. Davies, "The discovery of a galaxy-wide superwind from a young massive galaxy at redshift $z \sim 3$," *Nature* **436**, pp. 227–229, July 2005.
3. A. Weijmans, R. G. Bower, J. E. Geach, A. M. Swinbank, R. J. Wilman, P. T. de Zeeuw, and S. L. Morris, "Dissecting the Lyman α emission halo of LAB1," *MNRAS* **402**, pp. 2245–2252, Mar. 2010.
4. S. R. Furlanetto, J. Schaye, V. Springel, and L. Hernquist, "Mapping the Cosmic Web with Ly α Emission," *Astrophysical Journal Letters* **599**, pp. L1–L4, Dec. 2003.
5. C. Faucher-Giguère, A. Lidz, and L. Hernquist, "Numerical Simulations Unravel the Cosmic Web," *Science* **319**, pp. 52–, Jan. 2008.
6. J. Wolfe and D. Sanders, "Optical and environmental performance of durable silver mirror coatings fabricated at lnl," in *Optical Interference Coatings, Optical Interference Coatings*, p. TuF11, Optical Society of America, 2004.
7. S. C. Barden, J. B. Williams, J. A. Arns, and W. S. Colburn, "Tunable Gratings: Imaging the Universe in 3-D with Volume-Phase Holographic Gratings (Review)," in *Imaging the Universe in Three Dimensions*, W. van Breugel & J. Bland-Hawthorn, ed., *Astronomical Society of the Pacific Conference Series* **195**, pp. 552–+, 2000.
8. I. K. Baldry, J. Bland-Hawthorn, and J. G. Robertson, "Volume Phase Holographic Gratings: Polarization Properties and Diffraction Efficiency," *Publ. Astron. Soc. Pac.* **116**, pp. 403–414, May 2004.
9. R. D. Rallison, R. W. Rallison, and L. D. Dickson, "Fabrication and testing of large area VPH gratings," in *Society of Photo-Optical Instrumentation Engineers (SPIE) Conference Series*, E. Atad-Ettinger & S. D'Odorico, ed., *Society of Photo-Optical Instrumentation Engineers (SPIE) Conference Series* **4842**, pp. 10–21, Feb. 2003.
10. J. B. Oke, "Faint spectrophotometric standard stars," *Astronomical Journal* **99**, pp. 1621–1631, May 1990.
11. H. W. Epps, "Camera designs for the Keck Observatory LRIS and HIRES spectrometers," in *Society of Photo-Optical Instrumentation Engineers (SPIE) Conference Series*, D. L. Crawford, ed., *Presented at the Society of Photo-Optical Instrumentation Engineers (SPIE) Conference* **1235**, pp. 550–561, July 1990.
12. M. Shepherd, "Palomar autoguider." <http://www.astro.caltech.edu/~mcs/autoguider/index.html>.
13. R. C. Kennicutt, Jr., L. Armus, G. Bendo, D. Calzetti, D. A. Dale, B. T. Draine, C. W. Engelbracht, K. D. Gordon, A. D. Grauer, G. Helou, D. J. Hollenbach, T. H. Jarrett, L. J. Kewley, C. Leitherer, A. Li, S. Malhotra, M. W. Regan, G. H. Rieke, M. J. Rieke, H. Roussel, J. Smith, M. D. Thornley, and F. Walter, "SINGS: The SIRTf Nearby Galaxies Survey," *Publ. Astron. Soc. Pac.* **115**, pp. 928–952, Aug. 2003.